266 (2026) 214680

Contents lists available at ScienceDirect

Geoenergy Science and Engineering

journal homepage: www.sciencedirect.com/journal/geoenergy-science-and-engineering

Corrigendum

Corrigendum to "Rigorous numerical methodology and heat recovery analysis for modeling of direct use geothermal systems" [Geoenergy Sci. Eng. 247C, 213661]

Yuan Chen [a,*], Denis Voskov [a,b], Alexandros Daniilidis [a]

[a] Department of Geoscience & Engineering, TU Delft, Stevinweg 1, Delft, 2628 CN, Netherlands
[b] Department of Energy Science & Engineering, Stanford University, Stanford, CA, 94305, USA

The authors regret that during a post-publication review of the numerical model, we identified that rock thermal conductivity and rock heat capacity were not transferred properly for the ensemble run and were set to zero for the energy conservation equation. This resulted in earlier thermal breakthroughs because conductive heat transfer between the reservoir and the surrounding rock matrix was not accounted for.

After correcting the model and rerunning the simulations, we found that the correction affects only the reported numerical values. The overall trends, relative comparisons between scenarios, interpretations, and scientific conclusions presented in the paper remain unchanged. The inclusion of rock thermal conductivity primarily delays thermal breakthrough and therefore we extend the simulation time from 30 years to 80 years in base case to capture long-term thermal behavior. The sensitivity analysis indicates that the ranking of parameter importance remains consistent, whereas the magnitude of the importance scores increase after introducing the rock thermal conductivity and rock heat capacity.

We present the old and new results as follows,

Figure 2: Production temperature of different dx, dy and dz for a homogeneous reservoir

Old result:

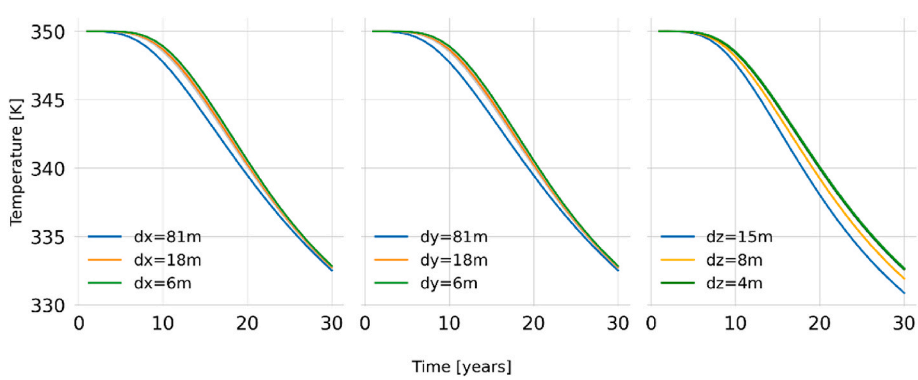

DOI of original article: https://doi.org/10.1016/j.geoen.2025.213661.
* Corresponding author.
E-mail address: y.chen-21@tudelft.nl (Y. Chen).

https://doi.org/10.1016/j.geoen.2026.214680

Available online 29 July 2026

New result:

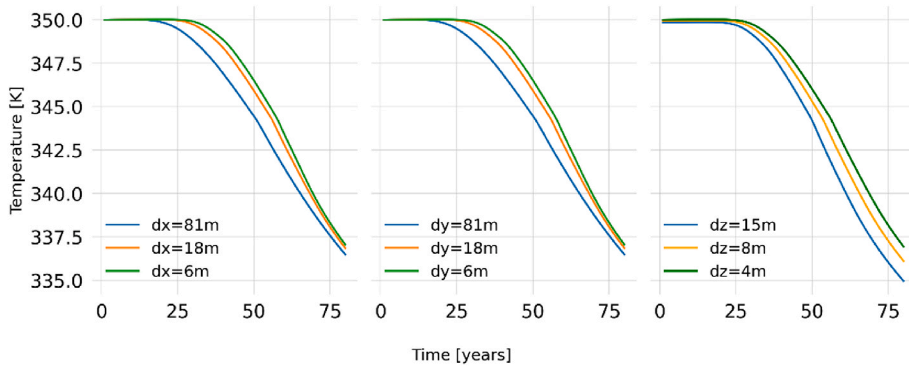

Implication: It requires longer simulation time to visualize the thermal breakthrough after including the rock heat capacity and rock conductivity. The simulation time changes from 30 years to 80 years.

Figure 3: RSS of the production temperature versus simulation time subject to different dx, dy and dz for different types of reservoirs. Different colors show the geological model types, the marker size indicates dx, dy and dz values with larger markers representing lower resolution.

Old result:

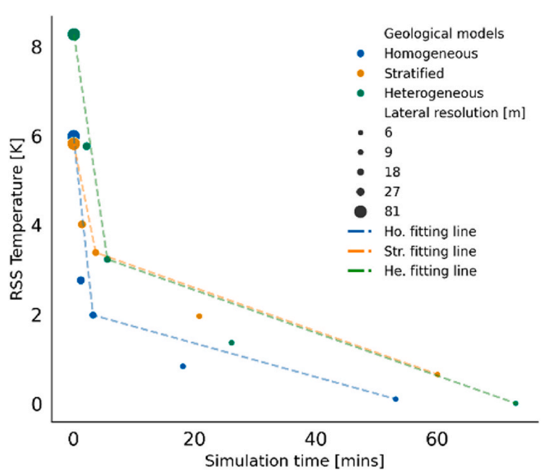

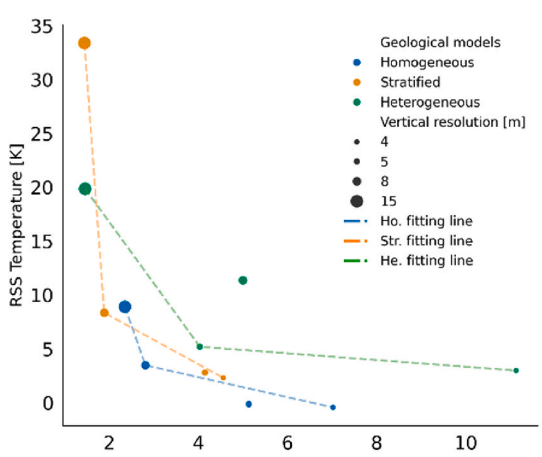

New result:

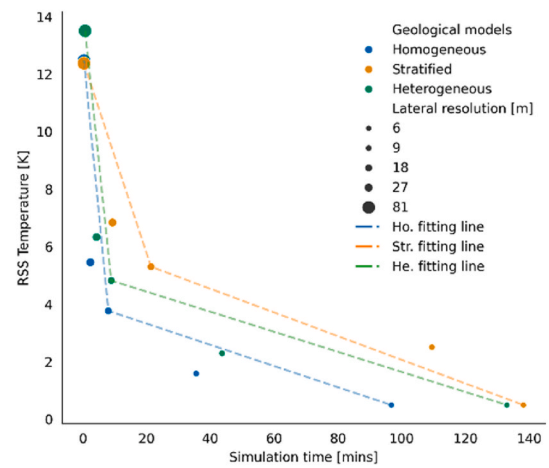

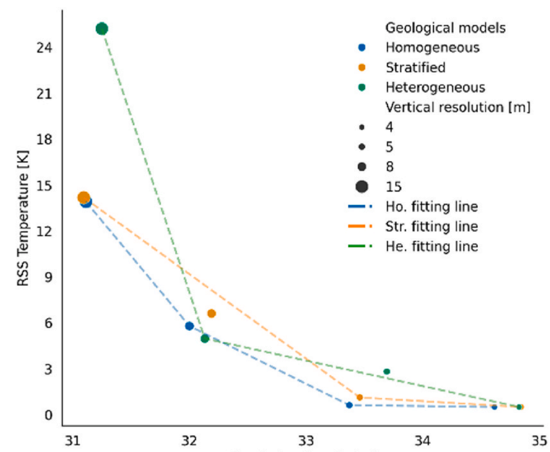

Implication: The simulation time becomes longer but the turning point with the optimal resolution does not change.

Figure 4: Cold plume extent volume ratio compared to the overall domain volume, subject to different dx, dy and dz for different types of geological models.

Old result:

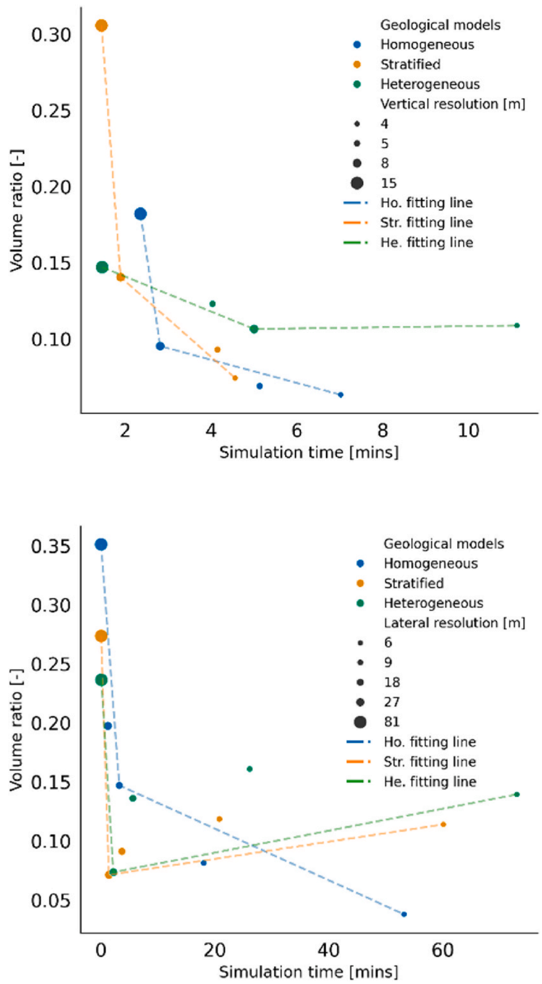

New result:

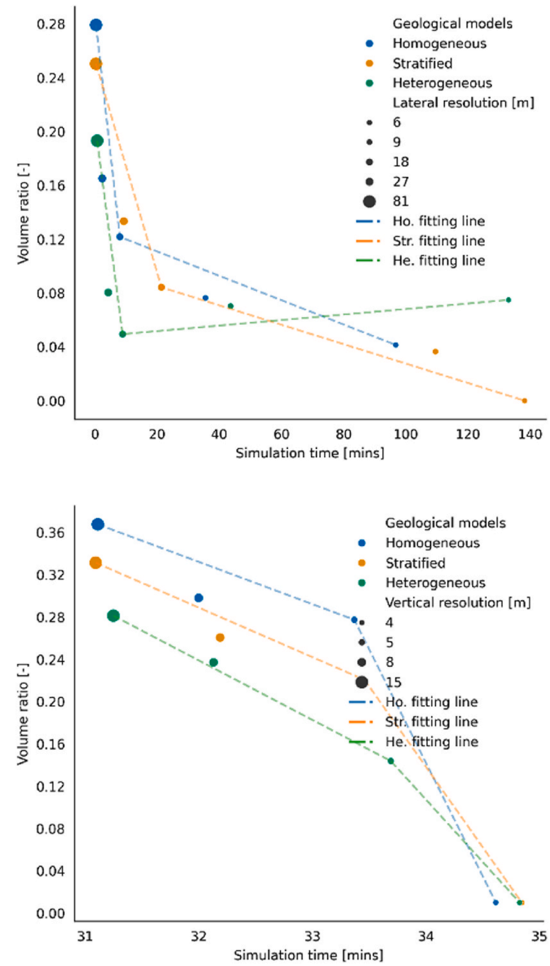

Implication: The simulation time becomes longer but the turning point with the optimal resolution does not change.

Table 2: Simulation results from different geological models.
Old result:

	Homogeneous			Stratified			Heterogeneous		
OBL resolution	Temp, RSS	Nonlinear, Iters.	Linear, per NI	Temp, RSS	Nonlinear, Iters.	Linear, per NI	Temp, RSS	Nonlinear, Iters.	Linear, per NI
8	10.5	132	11.41	14.7	146	13.02	24.1	147	13.11
16	3.0	131	11.15	2.7	135	12.66	2.9	137	12.65
32	0.7	120	11.11	0.6	122	12.40	0.8	123	12.74
64	0.2	115	11.39	0.2	117	12.42	0.2	118	12.97
128	0.05	112	11.54	0.04	115	12.74	0.04	115	13.37
Ref.	-	110	12.10	-	112	13.49	-	112	14.16

New result:

	Homogeneous			Stratified			Heterogeneous		
OBL resolution	Temp, RSS	Nonlinear, Iters.	Linear, per NI	Temp, RSS	Nonlinear, Iters.	Linear, per NI	Temp, RSS	Nonlinear, Iters.	Linear, per NI
8	10.3	293	10.3	7.1	299	14.76	11.3	311	16.52
16	3.6	289	15.80	3.3	297	15.05	3.5	298	16.49
32	0.85	280	15.82	0.93	284	15.12	0.80	280	16.61
64	0.21	273	16.17	0.20	273	15.28	0.22	275	16.89
128	0.05	268	16.38	0.05	270	15.56	0.06	272	17.12
Ref.	-	264	16.96	-	264	16.04	-	260	18.00

Implication: There are more time steps to make sure there is breakthrough, so the number of nonlinear iterations and the cost of iterations become larger, but the optimal physical resolution of interpolation table doesn't change.

Figure 5: The production temperature of different OBL physical resolution for the three geological models

Old result:

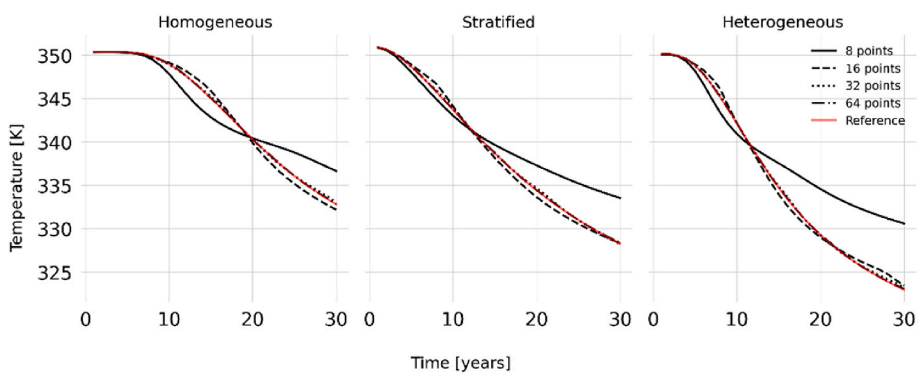

New result:

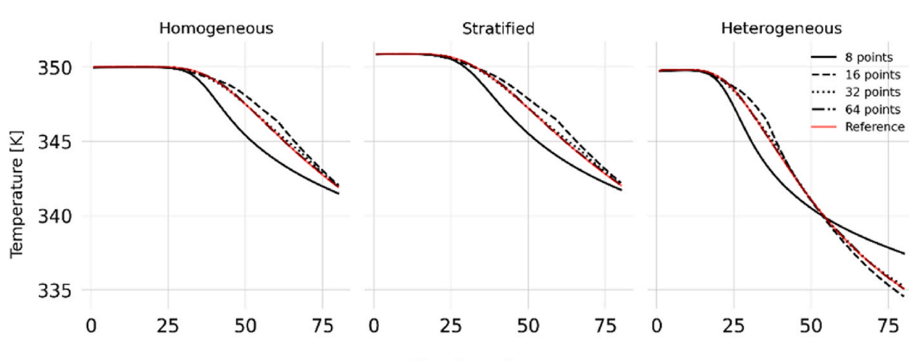

Figure 6: The efficiency and accuracy of simulation with variation in confining layers' dz: (a) The simulation time of the case with uniform and non-uniform dz at the confining layers; (b) Production temperature of a homogeneous model with uniform and non-uniform dz at the confining layers

Old result:

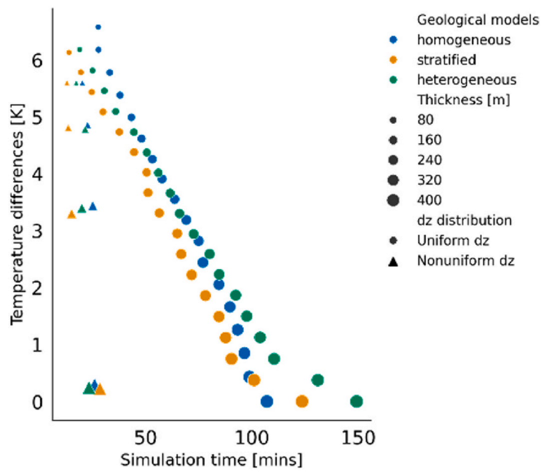

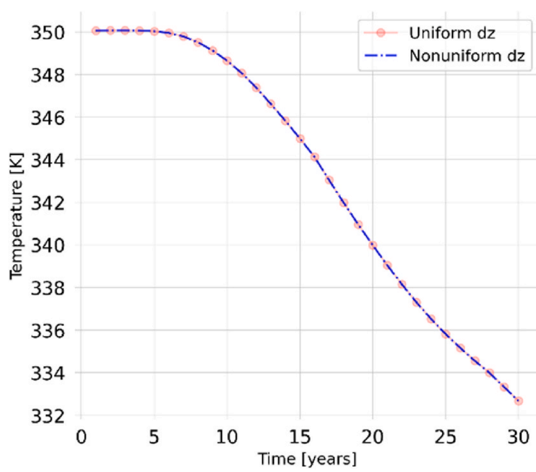

New result:

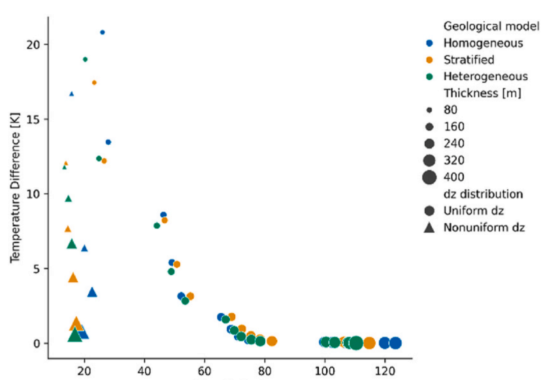

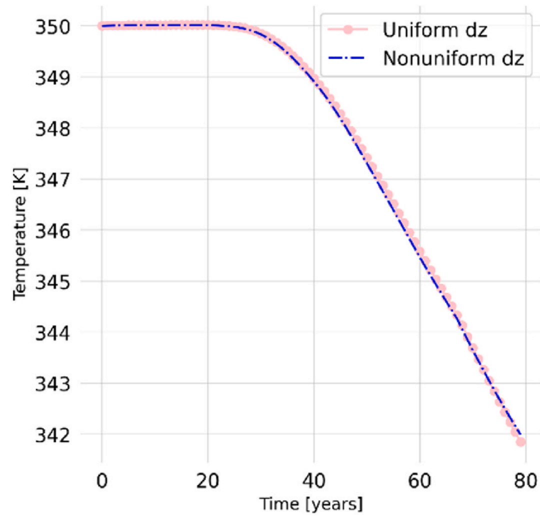

Figure 7: Temperature distribution of a homogeneous model with overburden and underburden layers at the well plane; the blue and red cylinder indicates the location of the injection well and production well respectively. The dashed green line shows the boundary between the confining layers and reservoir layers. An obvious heat flow by conduction happens between reservoir layers and confining layers

Old result:

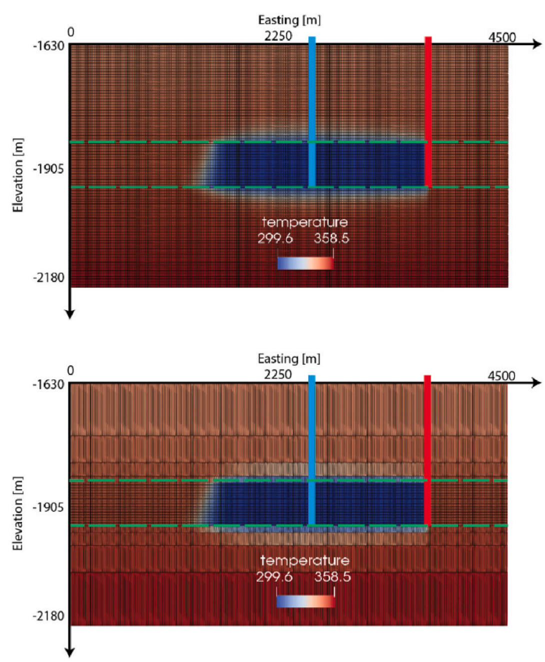

New result:

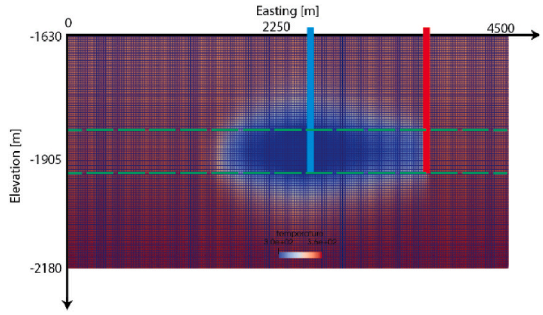

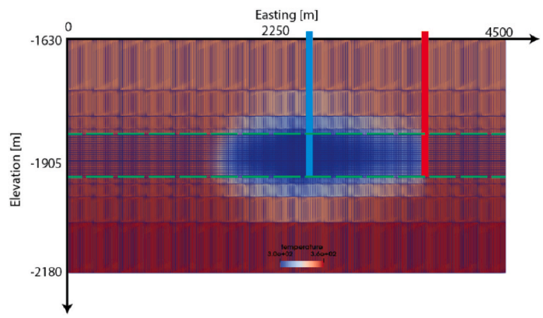

Table 3: Recoverable HIP of three types of the geological models when TOF is 80 years

Old result:

	HCA $[10^8 m^3]$	TAA $[10^8 m^3]$	Effective IA $[10^8 m^3]$	Recoverable HIP [PJ]
Homogeneous	4.78	4.87	6.10	88.27
Stratified	3.80	6.79	7.62	102.16
Heterogeneous	3.39	5.55	6.17	84.60

New result:

	HCA $[10^8 m^3]$	TAA $[10^8 m^3]$	Effective IA $[10^8 m^3]$	Recoverable HIP [PJ]
Homogeneous	18.1	10.6	18.1	171.93
Stratified	10.6	11.0	15.9	143.18
Heterogeneous	10.9	11.6	14.6	119.32

Implication: The time of flight has changed from 30 years to 80 years, so hydraulic-connected area (HCA) and thermal-affected area (TAA) become larger resulting in a larger effective influence area (IA).

Figure 8: Permeability, temperature and pressure distribution of the middle reservoir layer for homogeneous, stratified and heterogeneous reservoirs with the optimal numerical setup after 80 years simulation

Old result:

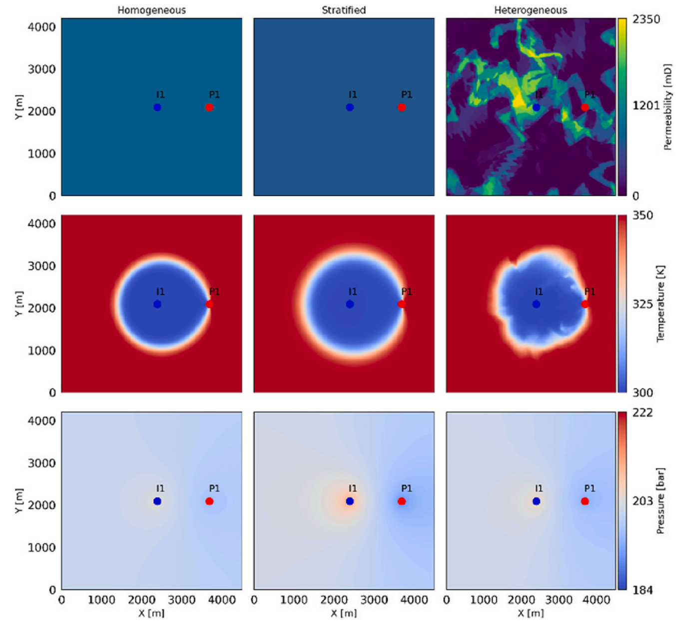

New result:

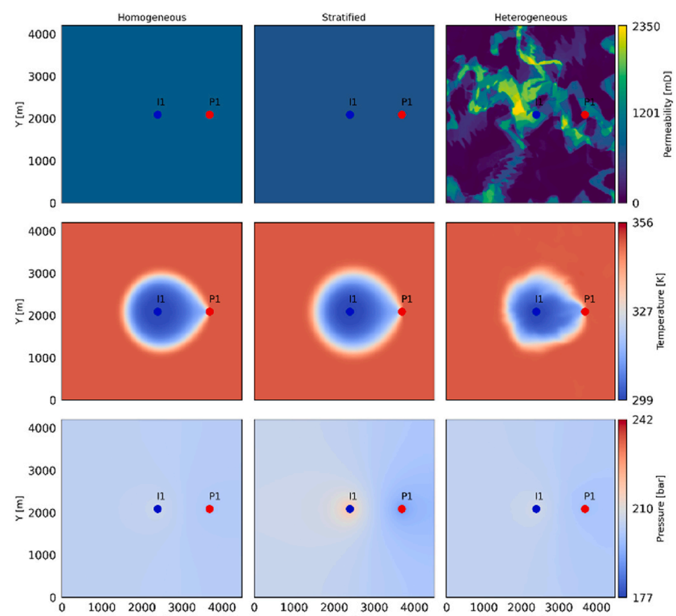

Figure 9: Hydraulic-Connected Area (HCA), Thermal-Affected Area (TAA) and effective IA (In columns) of different geological models (In rows). The blue and red tubes are injection and production wells respectively

Old result:

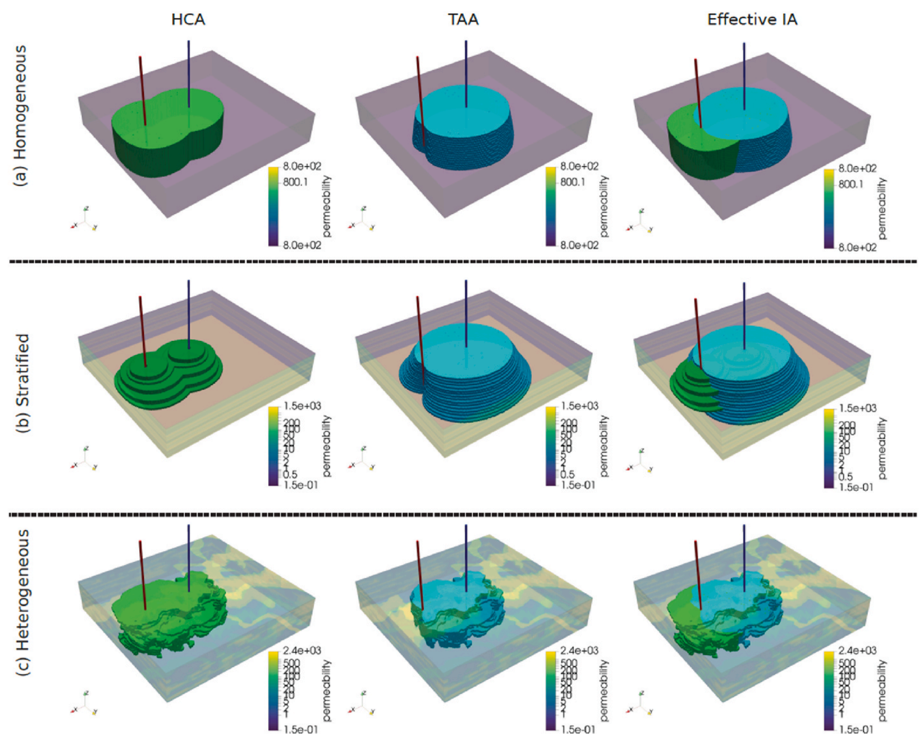

Implication: The new result includes the overburden and underburden layers because the heat recharge coming from the confining layers is more prominent compared to the previous setup with rock heat capacity and conductivity equals to 0.

Figure 10: Energy recovery factor of different geological models

New result:

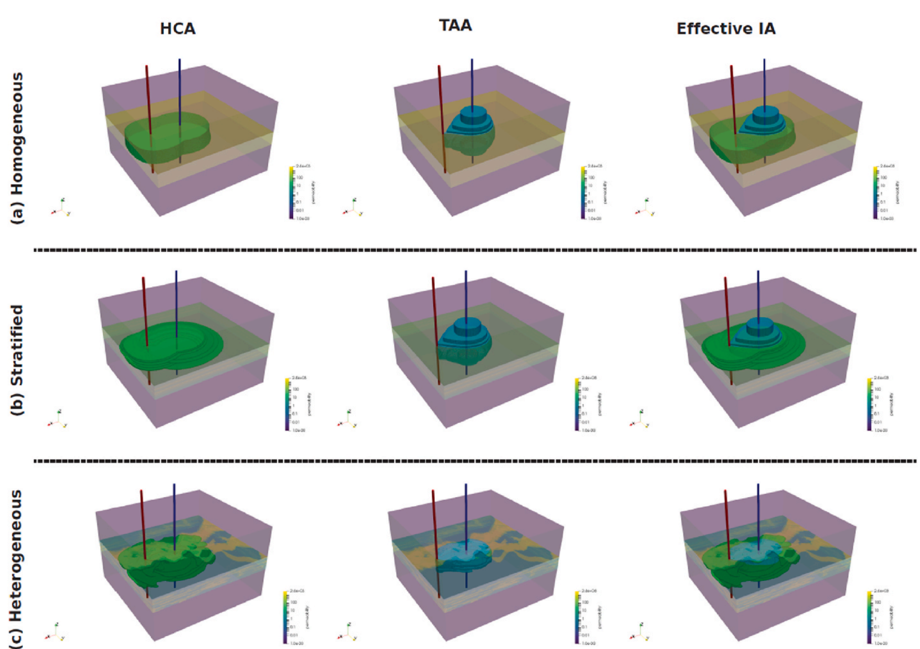

for varying PVI. Discharge rates change from 20 kg/s to 100 kg/s. Meanwhile the TOF has range between 1 years and 600 years. A non-linear equation is applied to fit (dashed line) pore volume injected (PVI) and HIP recovery factor for each geo-model, while a linear function is used to the fit dataset before thermal break-through (dotted line)

Old result:

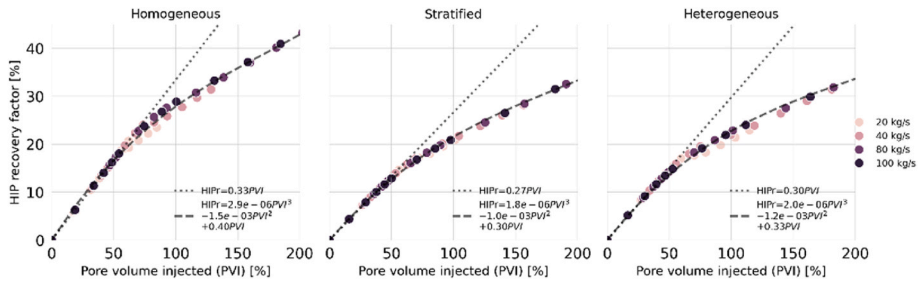

New result:

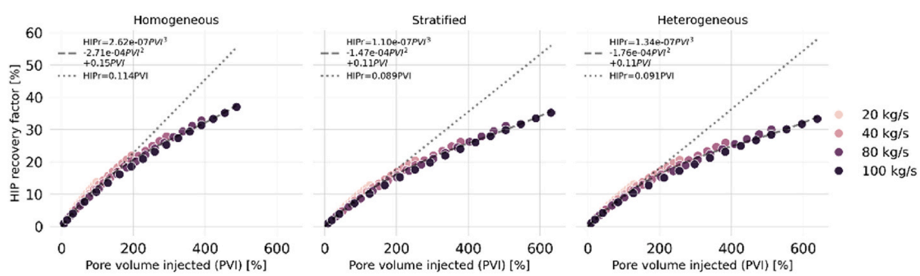

Implication: We need to run the simulation longer to get the thermal breakthrough, so the maximum simulation time changes from 240 years to 600 years.

Equation 27:

Old result:

$$T_{prod_t} \le 15\% \times (T_{prod_{t-0}} - T_{inj})$$

New result:

$$T_{prod_{t-0}} - T_{prod_t} \le 5\% \times (T_{prod_{t-0}} - T_{inj})$$

Implication: Because production temperature changes, it makes more sense to use small percentage to capture the small drop in production temperature.

Figure 11b: Recoverable HIP

Old result:

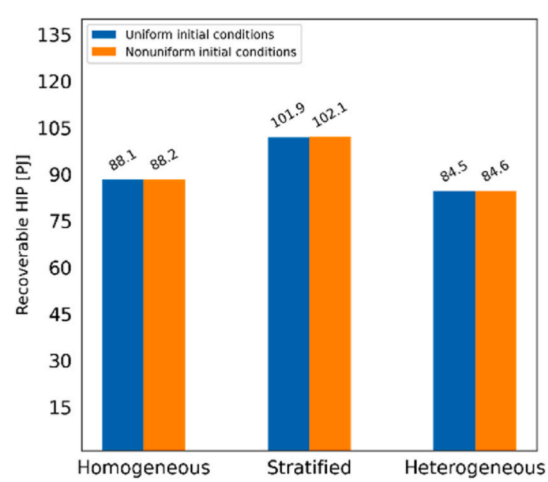

New result:

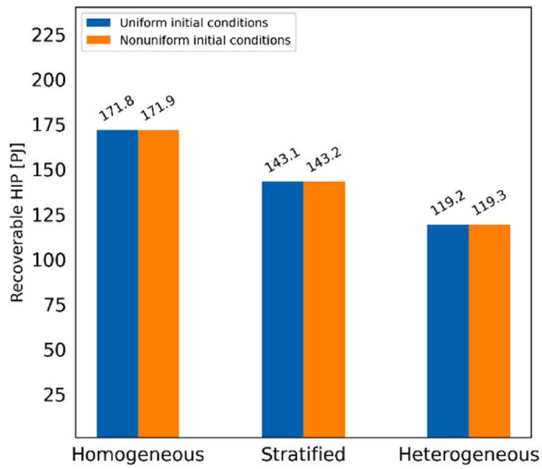

Figure 12: Temperature and injection well BHP for different types of geological models subject to different initial reservoir conditions

Old result:

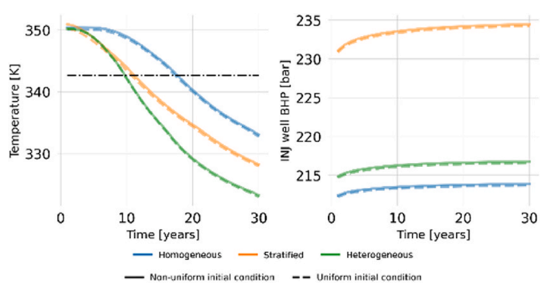

New result:

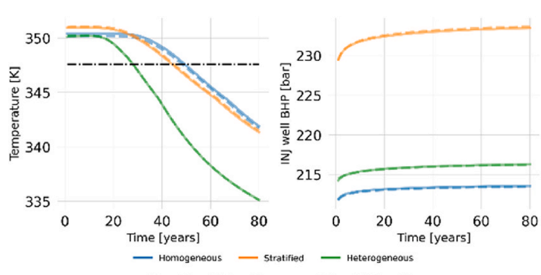

Figure 13: Temperature and injection well BHP for different types of geological models subject to different skin factors

Old result:

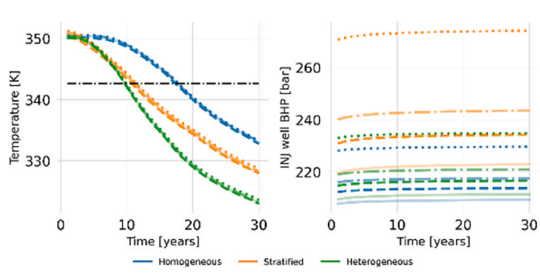

New result:

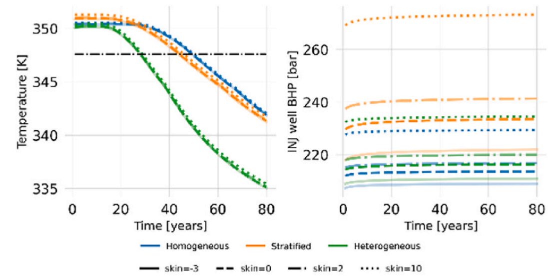

Figure 14: Temperature and injection well BHP for different types of geological models with/without gravity

Old result:

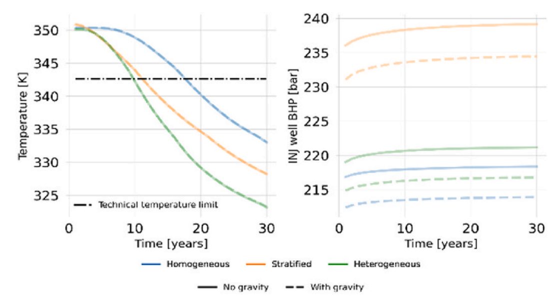

New result:

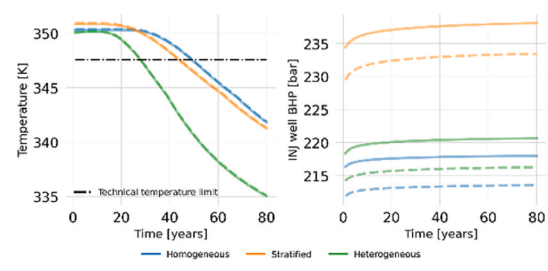

Figure 15: Temperature and injection well BHP for different types of geological models subject to different geological boundaries: open flow boundary and no flow boundary

Old result:

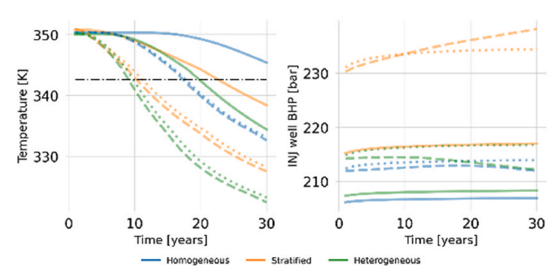

New result:

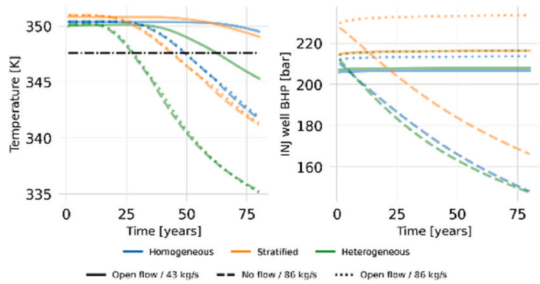

Figure 16: Temperature and injection well BHP for different types of geological models subject to different vertical-horizontal permeability ratio

Old result:

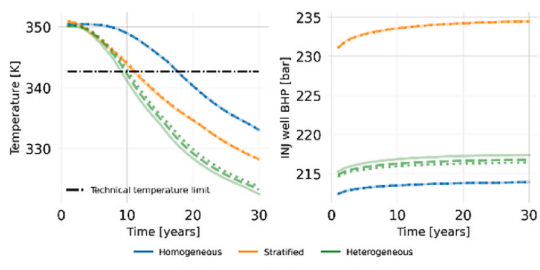

New result:

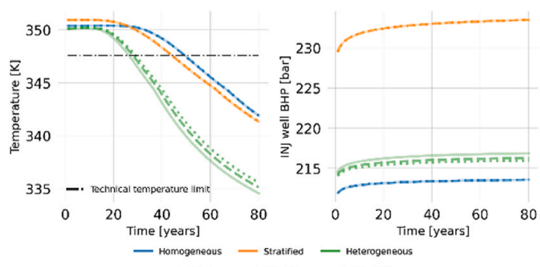

Figure 17: Temperature and injection well BHP for different types of geological models subject to different salinity

Old result:

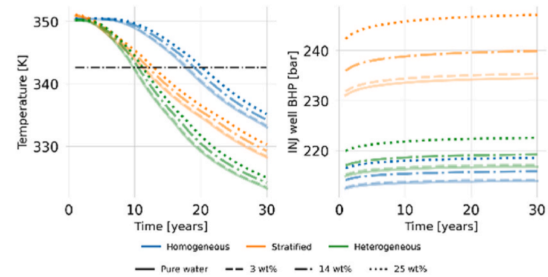

New result:

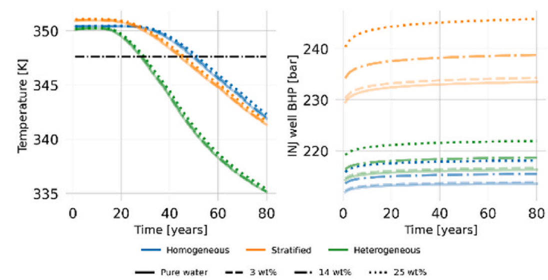

Figure 18: Temperature and injection well BHP for different types of geological models subject to constant density, viscosity

Old result:

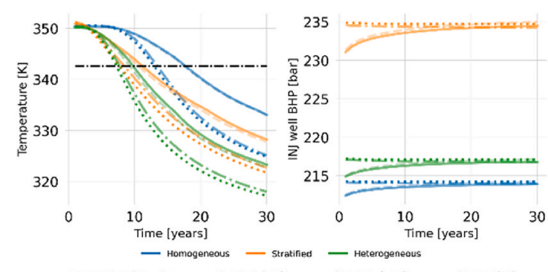

New result:

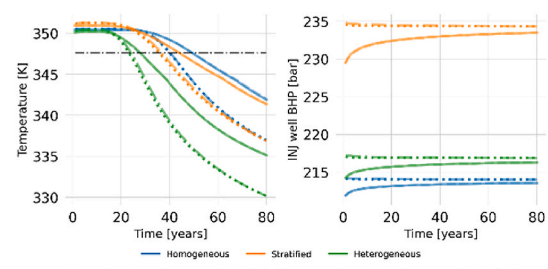

Figure 19: Pareto plot of main effect with CI taking production

temperature as a response

Old result:

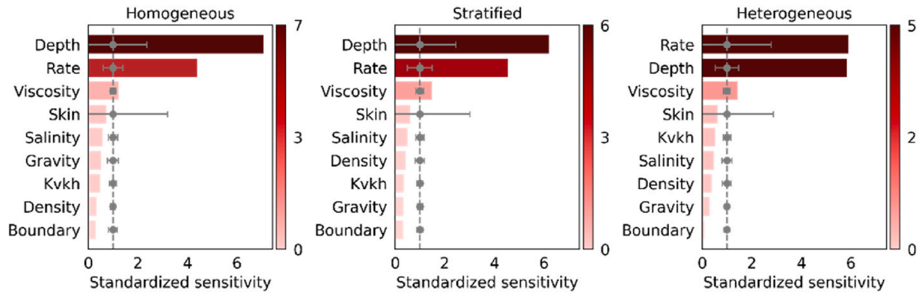

New result:

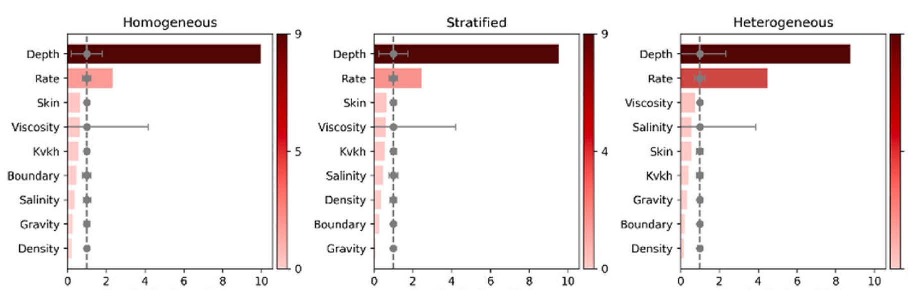

Figure 20: Pareto plot of main effect with CI taking injection well BHP as a response

Old result:

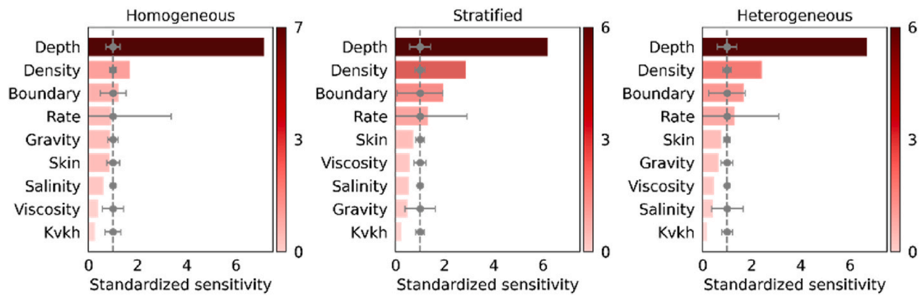

New result: